# The role of mantle ultrapotassic fluids in diamond formation

**Yuri N. Palyanov*, Vladislav S. Shatsky, Nikolay V. Sobolev, and Alexander G. Sokol**

Institute of Geology and Mineralogy, Siberian Branch of the Russian Academy of Sciences, Pr. Koptuyga 3, 630090 Novosibirsk, Russia

Edited by Ho-kwang Mao, Carnegie Institution of Washington, Washington, DC, and approved January 1, 2007 (received for review September 15, 2006)

**Analysis of data on micro- and nano-inclusions in mantle-derived and metamorphic diamonds shows that, to a first approximation, diamond-forming medium can be considered as a specific ultrapotassic, carbonate/chloride/silicate/water fluid. In the present work, the processes and mechanisms of diamond crystallization were experimentally studied at 7.5 GPa, within the temperature range of 1,400–1,800°C, with different compositions of melts and fluids in the $KCl/K_2CO_3/H_2O/C$ system. It has been established that, at constant pressure, temperature, and run duration, the mechanisms of diamond nucleation, degree of graphite-to-diamond transformation, and formation of metastable graphite are governed chiefly by the composition of the fluids and melts. The experimental data suggest that the evolution of the composition of deep-seated ultrapotassic fluids/melts is a crucial factor of diamond formation in mantle and ultrahigh-pressure metamorphic processes.**

high-pressure experiment

An important stage in solving problems of diamond genesis is constructing a clear physical model of diamond formation (1). One of the key parameters to be modeled is the composition of the diamond crystallization medium, with a fluid being largely considered as a crucial agent in diamond formation. It is generally agreed that the mantle media of diamond crystallization were volatile-saturated melts or fluids (1–7). Carbon-bearing fluids and carbonates could be sources of carbon, and the medium could have been saturated with it by redox reactions. Recent studies have been aimed at searching and examining fluid and fluid-containing inclusions in genetically different diamonds. Also, experiments have been performed to model the processes of diamond crystallization in the media compositionally corresponding to the inclusions. It is the combination of these two approaches that permits us to gain deeper insight into diamond genesis and to better understand the specific character of processes of deep-seated mineral formation.

Studies of mineral inclusions in diamonds have determined the main types of diamondiferous parageneses: ultramaffic, eclogitic (4, 8, 9), and intermediate websterite (10) and calc-silicate types (11). Some mineral inclusions, e.g., intergrowths of phlogopite with pyroxene (8, 12, 13) and phlogopite with calcite (14), are unambiguously evidence that K and $H_2O$ were present in the diamond-forming medium. It is pertinent to note that, as early as 30 years ago, neutron activation analysis of diamonds without visible inclusions, taken from three South African deposits, revealed a mixture of mostly K and of other components, which was interpreted as evidence of the presence of entrapped melt (15). Principally, more recent information has accrued from micro- and nano-inclusions in mantle-derived and metamorphic diamonds. Analysis of the composition of the inclusions in fibrous or cloudy mantle diamonds shows that, at the time of entrapment, the inclusion matter was a specific fluid whose composition belongs to one of the three main types: (*i*) a hydrous-silicic end-member that is rich in water, Si, Al, and K; (*ii*) a carbonatitic end-member that is rich in carbonate, Mg, Ca, Fe, K, and Na; and (*iii*) a brine (hydrous-saline end-member that is rich in Cl, K, and Na) (16–23). Despite wide compositional variations, all inclusions are enriched in K (24). Infrared spectroscopy applied to diamonds with such inclusions has revealed $H_2O$ and carbonates (16, 25), suggesting that the diamond crystallization medium was a supercritical fluid or melt (17, 26).

The discovery of microdiamonds in garnets and zircons from metamorphic rocks of the Kokchetav Massif (3) and subsequently in other ultrahigh-pressure (UHP) metamorphic terranes (27–32) is taken as evidence that the crustal rocks were subducted to considerable depths. FTIR microspectroscopy has revealed fluid inclusions in metamorphic diamonds (33); bulk chemical analyses of the Kokchetav microdiamonds demonstrated high contents of K and Cl (34). New results of studies of micro- and nano-inclusions in diamonds from UHP terranes (35–37) have indicated that the composition of diamondiferous water-bearing fluids was also ultrapotassic, with variations in carbonate, brine, and silicate components. The experiments in which the Kokchetav metamorphic rocks were used as the crystallization medium corroborated the governing role of the water-bearing fluid or melt in the process of the formation of UHP metamorphic diamonds (38, 39).

A specific role of alkalies in deep-seated parageneses was noted long ago (8). Mica and amphibole, appropriate to mantle compositions, are stable up to 6 GPa (40). However, primary amphibole inclusions have not yet been detected in kimberlitic diamonds. Clinopyroxene may be the fundamental solid host for K in most of the upper mantle and should be a good monitor of high K activity in the mantle (41). The first reports of K-rich pyroxenes in diamonds (8) supported the contention that their crystallization media were ultrapotassic melts/fluids (41). K-rich pyroxenes might form on the liquidus of a silicate magma mixed or coexisting with K-rich brine (42). Recent attention to chlorides is also due to new evidence of their participation in metasomatic processes in the mantle (43–46) and deep zones of the crust (47). Speculation of the possible nature of Cl in the mantle has also been recently reviewed (48).

Analysis of microinclusions has supplied the data from which the composition of the diamond-forming medium can be roughly considered as ultrapotassic carbonate/chloride/silicate/water. The review of data on experimental modeling of diamond formation (49) shows that the available experimental data are still too scarce to estimate the role of fluids of different composition in the processes of diamond formation. The few previous experiments on diamond crystallization in halide melts or halide-bearing systems are rather contradictory. Wang and Kanda (50) were the first to carry out studies on growth of diamond by using melts of alkaline halides at 6 GPa and 1,400–1,620°C for 5 h. They established that no diamond nucle-

Author contributions: Y.N.P., V.S.S., N.V.S., and A.G.S. designed research; Y.N.P. and A.G.S. performed research; A.G.S. contributed new reagents/analytic tools; Y.N.P., V.S.S., N.V.S., and A.G.S. analyzed data; and Y.N.P., V.S.S., N.V.S., and A.G.S. wrote the paper.

The authors declare no conflict of interest.

This article is a PNAS Direct Submission.

Abbreviations: FG, film growth; TGG, temperature-gradient growth; UHP, ultrahigh-pressure.

*To whom correspondence should be addressed. E-mail: palyanov@uiggm.nsc.ru.





www.pnas.org/cgi/doi/10.1073/pnas.0608134104

**Table 1. Experimental results at 7.5 GPa**

| Run *n* | *t*, °C | Time, h | Initial composition, wt % | | | Diamond nucleation | Mechanism Gr → Dm transformation | α Gr → Dm transformation, % | Diamond morphology | Metastable graphite |
|---|---|---|---|---|---|---|---|---|---|---|
| | | | KCl | $K_2CO_3$ | $H_2O$ | | | | | |
| 550/2 | 1,800 | 10 | 100 | — | — | — | — | 0 | — | — |
| 555/2 | 1,800 | 15 | 100 | — | — | — | — | 0 | — | — |
| 548/2 | 1,800 | 20 | 100 | — | — | + | FG | 2 | {111} | — |
| 557/2 | 1,600 | 20 | 100 | — | — | — | — | 0 | — | — |
| 1043B | 1,600 | 15 | 80 | 20 | — | + | FG, TGG | 100 | {111}, {100} | — |
| 1048B | 1,600 | 15 | 50 | 50 | — | + | FG, TGG | 100 | {111}, {100} | — |
| 1043A | 1,600 | 15 | 50 | 50 | — | + | FG, TGG | 100 | {111}, {100} | — |
| 1048A | 1,600 | 15 | 25 | 75 | — | + | FG, TGG | 100 | {111}, {100} | — |
| 559/2 | 1,600 | 15 | — | 100 | — | + | FG, TGG | 100 | {111}, {100} | — |
| 1036A | 1,550 | 15 | — | 100 | — | + | FG, TGG | 90 | {111}, {100} | — |
| 1036B | 1,550 | 15 | 24 | 76 | — | + | FG, TGG | 80 | {111}, {100} | — |
| 1053A | 1,500 | 15 | — | 100 | — | + | FG, TGG | 2 | {111}, {100} | — |
| 1053B | 1,500 | 15 | 50 | 50 | — | + | FG, TGG | 1 | {111}, {100} | — |
| 1035A | 1,400 | 15 | – | 100 | — | — | — | — | — | + |
| 1035B | 1,400 | 15 | 30 | 70 | — | — | — | — | — | + |
| 1060B | 1,600 | 15 | — | 81 | 19 | + | TGG | 6 | {111} | — |
| 1046B | 1,600 | 15 | — | 65 | 35 | + | TGG | 100 | {111} | — |
| 1045B | 1,600 | 15 | — | 37 | 63 | + | TGG | 100 | {111} | — |
| 1038B | 1,500 | 15 | — | 83 | 17 | + | TGG | <1 | {111} | + |
| 1054A | 1,500 | 15 | — | 65 | 35 | + | TGG | 4–5 | {111} | + |
| 1038A | 1,500 | 15 | — | 48 | 52 | + | TGG | 8 | {111} | + |
| 1062B | 1,500 | 15 | — | 10 | 90 | + | TGG | 70 | {111} | — |
| 1042A | 1,600 | 15 | 83 | — | 17 | + | TGG | 2 | {111} | + |
| 1060A | 1,600 | 15 | 68 | — | 32 | + | TGG | 4 | {111} | + |
| 1046A | 1,600 | 15 | 34 | — | 66 | + | TGG | 100 | {111} | — |
| 1042B | 1,600 | 15 | 31 | — | 69 | + | TGG | 100 | {111} | — |
| 745/2 | 1,600 | 15 | — | — | 100 | + | TGG | 95 | {111} | — |
| 1058A | 1,500 | 15 | 81 | — | 19 | — | — | 0 | — | + |
| 1054B | 1,500 | 15 | 65 | — | 35 | + | TGG | <1 | {111} | + |
| 1061A | 1,500 | 15 | 53 | — | 47 | + | TGG | 4 | {111} | + |
| 1062A | 1,500 | 15 | 9 | — | 91 | + | TGG | 70 | {111} | + |
| 1061B | 1,500 | 15 | — | — | 100 | + | TGG | 60 | {111} | — |
| 1085B | 1,500 | 15 | 40 | 36.5 | 23.5 | + | TGG | <1 | {111} | + |
| 1086A | 1,500 | 15 | 20.1 | 39.7 | 40.2 | + | TGG | 5 | {111} | + |
| 1086B | 1,500 | 15 | 39.1 | 20.1 | 40.8 | + | TGG | 2 | {111} | + |

α is the degree of graphite-to-diamond transformation. $\alpha = M_{Dm}/(M_{Dm} + M_{Gr})100$, where $M_{Dm}$ is the mass of obtained diamond and $M_{Gr}$ is the mass of residual graphite. Dm, diamond, Gr, graphite.

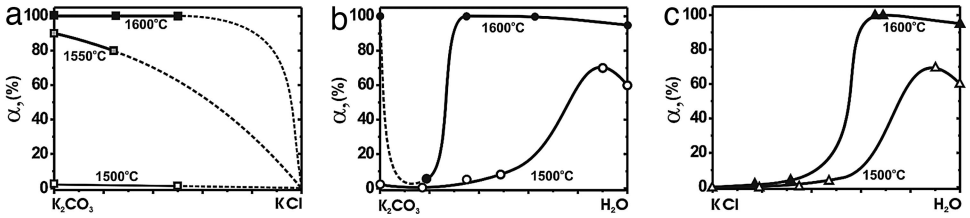


**Fig. 1.** Degree of graphite-to-diamond transformation [$\alpha = M_{Dm}/(M_{Dm} + M_{Gr})100$, where $M_{Dm}$ is the mass of obtained diamond and $M_{Gr}$ is the mass of residual graphite] as a function of the crystallization media composition ($P$ = 7.5 GPa, $\tau$ = 15 h). (*a*) $K_2CO_3$/KCl/C system. (*b*) $K_2CO_3/H_2O$/C system. (*c*) KCl/$H_2O$/C system.

ation occurred under these conditions, although diamond layers grown on seeds were very small, only ≈1 μm thick. A more considerable growth was observed in the $K_2CO_3$/KCl/C system, with the temperature range of 1,050–1,260°C at 7–7.7 GPa in 60-min experiments (51). Spontaneous crystallization of diamond in the KCl/C system at 7–8 GPa and 1,500–1,700°C in experiments lasting 10 s to 40–60 min was reported in ref. 52. To our knowledge, there are no experimental data on diamond crystallization in water-containing chloride or chloride-carbonate systems.

The present study is aimed at establishing the mechanisms and regularities of diamond crystallization with reference to the composition of ultrapotassic melts and fluids[†] in the system KCl/$K_2CO_3$/$H_2O$/C at the mantle pressures and temperatures.

## Results

The results of the experiments performed with different starting mixtures are summarized in Table 1. Diamond growth on seeds was observed with the first series of experiments, in 10- and 15-h-long experiments with the use of KCl at 1,800°C and 7.5 GPa, whereas spontaneous crystallization of octahedral diamonds was established only in the 20-h experiment. Diamond crystallized from carbon solution in a KCl melt. At 1,600°C, no melting was established in the KCl/C system, which agrees with ref. 50. However, some diamond growth on seeds took place, and we believe that this was due to the presence of microquantities of a fluid phase formed as a result of atmospheric gases adsorbed on the initial reagents (53).

There is no difference in the intensity and character of diamond crystallization in the $K_2CO_3$ versus carbonate-chloride melts, with 25 and 50 wt % KCl at 1,600°C, and with the degree of graphite-to-diamond transformation equal to 100%. When a chloride-carbonate melt (80% KCl and 20% $K_2CO_3$) was used, KCl crystallized on the bottom of the ampoule, and a carbonate-chloride melt with the components proportion of ≈1:1 was in contact with graphite. Experiments at 1,550 and then 1,500°C led to a drastic decrease in the degree of graphite-to-diamond transformation ($\alpha$), indicating that carbonate melt is more effective as a diamond-forming medium than carbonate-chloride melt (Fig. 1*a*). At 1,400°C in experiments with $K_2CO_3$ and $K_2CO_3$ + KCl (30/70), no diamond nucleation occurred for 15 h; in both cases, slight growth of diamond and metastable graphite was observed on diamond seeds.

In this series of experiments, diamond crystallized by film growth (FG) and temperature-gradient growth (TGG) mechanisms. In the first case, the driving force for the crystallization was a difference in solubility of graphite and diamond in the melt, with constant $P$,$t$ (pressure and temperature). In the second case, diamond crystallization was driven by the difference in solubility of carbon at the different temperatures within the thermal gradient field. During the FG crystallization, diamond nucleation occurred at the graphite-melt boundary, whereas in the TGG process, growth took place either on walls of the Pt ampoule in the low-temperature zone (heterogeneous nucleation) or directly in the melt (homogeneous nucleation). The FG and TGG mechanisms were first described in ref. 54 for metal–carbon systems. Subsequently, it was established that these mechanisms are also typical of diamond crystallization in nonmetal melts, e.g., of carbonates (55), carbonate with silicates (56), sulfur (57), and sulfides (58). In dry melts of the KCl/$K_2CO_3$/C system, diamonds crystallized mainly by the FG mechanism, and only few diamonds (<1%) crystallized by TGG. The degree of graphite-to-diamond transformation ($\alpha$) as a function of temperature is presented in Fig. 1*a*. It demonstrates two distinct trends: (*i*) a decrease in temperature in the range of 1,600–1,400°C leads to a drastic drop in $\alpha$ from 100% to zero; and (*ii*) an addition of KCl to $K_2CO_3$ results in a decrease in intensity of diamond formation. The latter was most clearly demonstrated in experiment 1053A,B at 1,500°C; the number of diamond crystallization centers at the graphite-$K_2CO_3$ melt interface was 7 $mm^{-2}$, and in the case of the melt KCl:$K_2CO_3$ (50:50), it was 3 $mm^{-2}$. In the whole range of compositions, FG crystallization of diamond can be considered homogeneous, because diamonds nucleated in the melt.

Diamond crystallization in the system $K_2CO_3/H_2O/CO_2$/C was studied earlier at 5.7 GPa and 1,150–1,420°C with relatively low concentrations of water (59, 60). However, to make a correct comparison of different compositions in the system KCl/$K_2CO_3$/$H_2O$/C at equal $P$,$t$, and run duration ($\tau$), we performed additional experiments. At 1,600°C, addition of water to $K_2CO_3$ principally changes the mechanism of diamond nucleation. In pure $K_2CO_3$, mainly an FG mechanism operates (run 559/2) with $\alpha = \alpha_{FG} + \alpha_{TGG} = 100\%$, with $\alpha_{FG} > 99\%$ and $\alpha_{TGG} < 1\%$. Addition of water completely terminates FG ($\alpha_{FG} = 0$), leaving only TGG acting, with $\alpha = \alpha_{TGG}$ being very low (run 1060B). Further increase in $H_2O$ content results in an abrupt increase in $\alpha$ (Fig. 1*b*). With a temperature decrease to 1,500°C, the degree of graphite-to-diamond transformation decreases, and the amount of metastable graphite increases (Fig. 1*b*). With an increase in water content, the heterogeneous diamond nucleation is supplemented by the homogeneous process in the essentially aqueous fluid. Remarkably, in dry $K_2CO_3$ and $K_2CO_3$/KCl melts, diamond crystallizes in the form of cubo-octahedra (Fig. 2*a*) by both FG and TGG, and the addition of water results in the growth of octahedra.

In the system KCl/$H_2O$/C at 7.5 GPa and 1,600°C, with 17 and 32 wt % $H_2O$, spontaneous diamond crystals formed by TGG, and significant amounts of large (up to 1.5 mm) crystals of metastable graphite were found. With a further increase in $H_2O$ content, to 66 and 69 wt %, the graphite-to-diamond transformation reached 100%, with no metastable graphite formed. In pure water, the mechanism of diamond nucleation was the same, but not all graphite was transformed into diamond ($\alpha$ = 95%). It should be noted that data on diamond formation in the system $H_2O$/C are in agreement with previous studies (61–64). A decrease in temperature to 1,500°C resulted in a decrease in the rate of diamond

[†]Under conditions of complete miscibility between water-containing melts and aqueous fluids, we will conventionally refer to water-poor and water-rich compositions as melts and fluids, respectively.

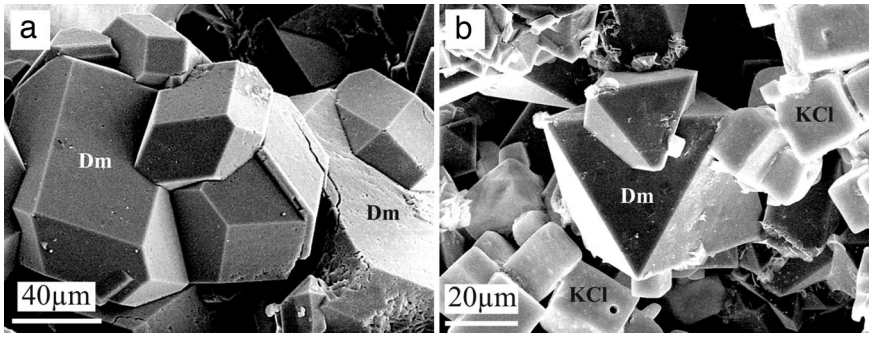


**Fig. 2.** Scanning electron micrographs of diamonds. (*a*) Cubo-octahedral diamonds synthesized in the $K_2CO_3$/KCl/C system (run 1053B). (*b*) Octahedral diamonds synthesized in the KCl/$H_2O$/C system (run 1046A).

formation, but the general trend of behavior of $\alpha$ as a function of composition remained the same (Fig. 1*c*). With 19 wt % $H_2O$ added to KCl, no diamond nucleation was observed, and only metastable graphite was present in the capsule. An increase in water content in the KCl/$H_2O$ system led first to heterogeneous nucleation of diamond and gradual growth of $\alpha$ (Fig. 1*c*); then, homogeneous nucleation was observed in the essentially aqueous fluid. In general, at similar concentrations of $H_2O$, carbonate melts/fluids are characterized by higher values of $\alpha$ than the chloride melts/fluids. In all experiments with water/chloride compositions and in pure water, diamonds crystallized exclusively in the form of octahedra (Fig. 2*b*).

Three control experiments with starting compositions corresponding to the points inside the KCl/$K_2CO_3$/$H_2O$ triangle were performed at 1,500°C (Table 1). In all these experiments, heterogeneous spontaneous nucleation of diamond and formation of metastable graphite were established. The degree of graphite-to-diamond transformation ($\alpha$) depended significantly on the medium composition. The minimal value of $\alpha < 1$ was established at 23.5% $H_2O$ and an approximately equal ratio of KCl/$K_2CO_3$. In run 1086, the composition in capsules A and B differed in the KCl/$K_2CO_3$ ratio (1:2 and 2:1, respectively) having the same $H_2O$ content (≈40%). The degree of graphite-to-diamond transformation differed markedly, with $\alpha_A = 5\%$ and $\alpha_B = 2\%$. Taken as whole, the results of the control experiments are in good agreement with the data for binary compositions.

Fig. 3 summarizes the main regularities of crystallization of diamond and metastable graphite in the system KCl/$K_2CO_3$/$H_2O$/C at temperatures of 1,600 and 1,500°C. Therein, regions of homogeneous and heterogeneous diamond nucleation and zones of no nucleation are marked. The variation of the degree of graphite-to-diamond transformation ($\alpha$) at constant $P$ = 7.5 GPa, $t$ = 1,500°C, and $\tau$ = 15 h, depicted on the composition ternary diagram, is shown in Fig. 4.

## Discussion and Conclusions

Analysis of the experimental data permits establishing the following main regularities of diamond crystallization in the KCl/$K_2CO_3$/$H_2O$/C system.

1. In dry chloride, carbonate, and carbonate-chloride melts, diamond crystallizes mainly by the FG mechanism. The reactivity of the melts with respect to the nucleation of diamond decreases in the following sequence: $K_2CO_3$ > $K_2CO_3$ + KCl ≫ KCl. Water addition leads to a change of diamond crystallization mechanism from FG to TGG.
2. In carbonate-chloride aqueous melts and highly aqueous fluids, diamond crystallizes exclusively by TGG, with the carbonate/water media being more active than the chloride/water ones. Increasing water content in the subsystems KCl/$H_2O$ and $K_2CO_3$/$H_2O$ enhances diamond formation, and the heterogeneous diamond nucleation is supplemented with a homogeneous process. In the $H_2O$-rich fluids, the degree of graphite-to-diamond transformation $\alpha$ is subject to the following rule: $\alpha(H_2O + K_2CO_3) \approx \alpha(H_2O+KCl) > \alpha(H_2O)$.
3. Diamond morphology is sensitive to changes in composition of crystallization medium. In carbonate-chloride water-containing systems and $H_2O$, diamond crystallizes exclusively in the form of octahedra. In dry melts of $K_2CO_3$ and $K_2CO_3$/KCl, the growth form of diamond is cubo-octahedra. By integrating results from other studies (61), one can infer that the morphology of diamonds crystallized in melts of $K_2CO_3$ and $K_2CO_3$ + KCl tends to change from octahedral to cubo-octahedral as $P$,$t$ parameters move away from the line of graphite–diamond equilibrium.
4. The appearance of metastable graphite in the field of thermodynamic stability of diamond in the system of the present study depends on the temperature and composition of the crystallization medium. At 7.5 GPa, a decrease in tempera-

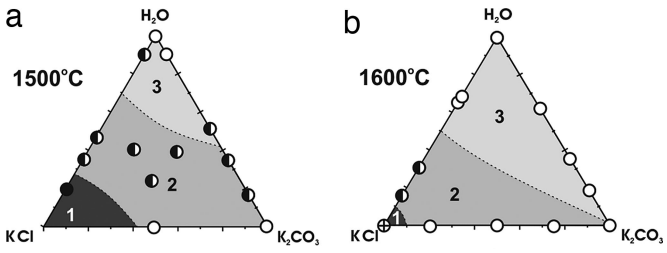


**Fig. 3.** Effect of the KCl/$K_2CO_3$/$H_2O$/C system composition on diamond and graphite crystallization at $P$ = 7.5 GPa and $\tau$ = 15 h. (*a*) 1,500°C. (*b*) 1,600°C. 1, no diamond nucleation; 2, heterogenous diamond nucleation; 3, homogeneous and heterogenous diamond nucleation; half-filled circles, joint crystallization of diamond and metastable graphite; open circles, only diamond crystallization; filled circles, only graphite crystallization; circles with cross, no crystallization of graphite or diamond.

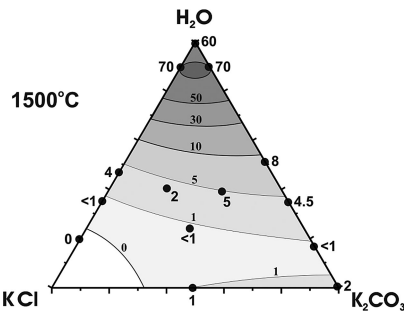


**Fig. 4.** Generalized diagram of the degree of graphite-to-diamond transformation ($\alpha$) in the KCl/$K_2CO_3$/$H_2O$/C system at $P$ = 7.5 GPa, $t$ = 1,500°C, and $\tau$ = 15 h. The values of $\alpha$ are given by numbers.

ture leads to the appearance of metastable graphite in all subsystems. At constant temperature, the intensity of formation of metastable graphite changes substantially depending on the composition of crystallization medium in the succession: $KCl + H_2O > K_2CO_3 + H_2O > K_2CO_3 + KCl > H_2O$.

The established sequences in crystallization of diamond and metastable graphite in the $KCl/K_2CO_3/H_2O/C$ system, have been used to: (*i*) model the composition of mantle-derived ultrapotassic fluid; and (*ii*) prove the drastic changes in the intensity of diamond formation, depending on the composition of crystallization medium and temperature, which implies a considerable change in carbon solubility. As applied to natural diamond formation processes, the FG mechanism should act similarly to the experiments, being restricted by the conditions of existence of dry melt and graphite as a source of carbon. The TGG mechanism observed in experiments is not possible in nature, because such temperature gradients are impossible. However, it is possible that similar TGG may occur, in which the driving force of diamond crystallization is a change of supersaturation caused by temperature drop, change of fluid composition, and/or redox reactions. It is hardly possible to suppose that, in the mantle and with UHP metamorphic processes, temperature could drastically change and, moreover, that temperature gradients could be great enough to provide diamond nucleation. It is typically assumed that elemental carbon is released during redox processes (2, 3, 65, 66). Experimentally, this possibility was demonstrated in reactions involving carbonates (67–71). The results of the present study show that the driving force for precipitating elemental carbon could be a change in concentrations of main components of chloride/carbonate/water fluid. The change in mechanisms of diamond crystallization and the drastic dependence of the processes of diamond formation on composition, as determined by the present study, suggest that the evolution of fluid composition is the main important factor responsible for spontaneous diamond nucleation at constant pressure and temperature.

The impact of the evolution of fluid composition is exemplified by diamond formation in UHP metamorphic rocks of the Kokchetav complex, as well as in mantle-derived kimberlitic diamonds. Inclusions of K- and P-rich silicate glass in diamonds from biotite gneisses and inclusions of high-K C/O/H fluid in diamonds from dolomitic marbles were identified (36, 37). A high density of diamond nucleation centers and morphological features are evidence for high supersaturation in the crystallization medium. Because the model of quickly changing temperature or pressure is not appropriate for UHP complexes, the driving force of diamond crystallization can be the change of chemical composition of medium.

Geochemical features of diamondiferous metamorphic rocks indicate that they experience partial melting (72, 73). The proof is the occurrence of melt inclusions in diamonds from gneisses (37), as well as globules of complex composition in garnets of dolomitic marbles (74). The presence of K-bearing pyroxenes, as well as lamellae of phengite and potassium feldspar in garnet-pyroxene rocks and dolomitic marbles indicate that, at the peak of metamorphism, these rocks were in equilibrium with high-K fluids. Being in equilibrium with dolomitic marbles, the fluid had essentially water/carbonate composition, and in equilibrium with gneisses, the fluid had essentially water/silicate composition. Subducted crustal rocks were the possible source of high-K fluids participating in diamond formation (75). The fact that at present these rocks are depleted in potassium may be explained by the removal of high-K fluids at one of the stages in the metamorphic evolution of rocks.

Because compositions of diamond-forming fluids in metamorphic and kimberlite diamonds are supposedly similar (36, 37, 18–20), one may assume that the model of the evolution of the fluid composition as the driving force of diamond crystallization may have broader implications. One of the evidences of possible variations of the composition of fluid in kimberlite diamonds may be the wide range of K contents in pyroxenes entrapped during diamond growth (8, 13, 76–78). Other direct evidences of significant variations of fluid composition during diamond crystal growth are presented in refs. 19 and 79.

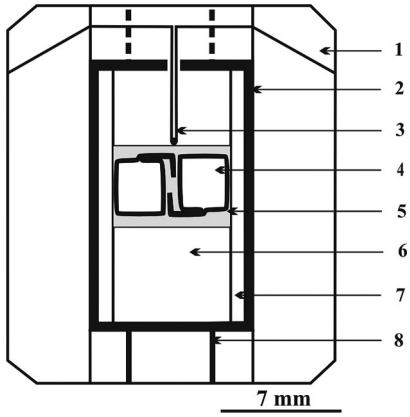


**Fig. 5.** High-pressure experimental cell for diamond crystallization in the $KCl/K_2CO_3/H_2O/C$ system. 1, $ZrO_2$ container; 2, cylindrical graphite heater; 3, $PtRh_6/PtRh_{30}$ thermocouple; 4, Pt capsules; 5, CsCl; 6, $ZrO_2$; 7, MgO; 8, Mo leads.

The composition of melts/fluids in a deep process significantly depends on various factors. If, at the time of melting of rocks, the pressure was below the second critical point (2 cP), the near-solidus liquid was carbonatitic, and any coexisting fluid was aqueous. At $P > P2$ cP, as melting degree increased, the fluid/melt composition should continuously vary between end-members, from aqueous through carbonatitic to carbonate/silicate liquids (6). Recent experimental studies (6, 80) show that such change of the fluid/melt composition took place in systems with compositions corresponding to mantle rocks. This process might have initiated spontaneous crystallization of diamond. The change of fluid composition (e.g., enrichment in carbonates or chlorides) might cause the cocrystallization of diamond and metastable graphite, leading to the formation of diamonds with graphite inclusions and graphite-coated diamonds. Some morphological features of diamonds also could be due to changes in composition of the crystallization medium. For example, the evolution of composition from carbonate/chloride melt to aqueous fluid could change the stable growth form of diamond from cubo-octahedral to octahedral, with the formation of a regeneration of morphology.

With this study, it has been established experimentally that diamond nucleation mechanisms, as well as the intensity of crystallization of diamond and metastable graphite, depend essentially on the composition of fluids and melts in the system $KCl/K_2CO_3/H_2O/C$ at constant pressure and temperature. This observation permits us to fortify the concept of the evolution in the composition of mantle-derived ultrapotassic fluids/melts as one of the main factors governing the nucleation and growth of diamond, as well as the formation of metastable graphite in the mantle and UHP metamorphic processes.

## Methods

Experiments were carried out by using a Multianvil, high-pressure apparatus of a "split-sphere" type (81). A high-pressure cell in the form of tetragonal prism, $19 \times 19 \times 22$ mm in size, is shown in Fig. 5. The temperature was measured in each experiment by using a PtRh30/PtRh6 thermocouple. Details on the pressure and temperature calibration and accuracy of the measurements are given in ref. 61. The starting materials were

a graphite disk (99.99% purity), $K_2CO_3$, KCl of purity not <99.9%, and distilled water. The initial reagents and cubo-octahedral diamond seed crystals were loaded into Pt capsules, which were sealed by arc welding. In each capsule, the mass of the graphite disk was 11.8 mg, and the total mass of solvent was 18 mg. To determine the effect of the medium composition on diamond crystallization more precisely, with each experiment, we used two capsules with different compositions located symmetrically with the high-pressure cell so that they would be subjected to the exact same $P$ and $t$ (see Fig. 5).

We thank Y. Borzdov, A. Khokhryakov, and I. Kupriyanov for their assistance throughout the study and Prof. L. A. Taylor for useful remarks and suggestions that helped to improve the manuscript. This work was supported by Russian Foundation for Basic Research Grants 04-0564236 and 06-05–64576 and Russian Foundation for Scientific Schools Grant NSH-5123.2006.5.

1. Navon O (1999) in *Proceedings of the Seventh Kimberlite Conference, Cape Town*, eds Gurney JJ, Gurney JL, Pascoe MD, Richardson SH (Red Roof Design, Cape Town, South Africa), pp 584–604.
2. Haggerty SE (1986) *Nature* 320:34–38.
3. Sobolev NV, Shatsky VS (1990) *Nature* 343:742–746.
4. Harris JW (1992) in *Properties of Natural and Synthetic Diamond*, ed Field JE (Academic, London) pp 345–389.
5. Boyd SR, Pineau F, Javoy M (1994) *Chem Geol* 116:29–42.
6. Wyllie PJ, Ryabchikov ID (2000) *J Petrol* 41:1195–1206.
7. Taylor LA, Anand M (2004) *Chem Erde* 64:1–74.
8. Sobolev NV *Deep-Seated Inclusions in Kimberlites and the Problem of Upper Mantle Composition*, trans Boyd FR (1977) (Amer Geophys Union, Washington DC).
9. Meyer HOA (1987) in *Mantle Xenoliths*, ed Nixon HP (Wiley, New York), pp 501–523.
10. Sobolev NV (1983) *Zap Vsesoyuznogo Min Obshch* 112:389–398.
11. Sobolev NV, Yefimova ES, Lavrentyev YG, Sobolev VS (1984) *Dokl Akadem Nauk SSSR* 274:130–135.
12. Prinz M, Manson DV, Hlava PF, Keil K (1975) *Phys Chem Earth* 9:797–815.
13. Sobolev NV, Yefimova ES, Channer DMD, Anderson PFN, Barron KM (1998) *Geology* 26:971–974.
14. Sobolev NV, Kaminsky FV, Griffin WL, Yefimova ES, Win TT, Ryan CG, Botkunov AI (1997) *Lithos* 39:135–157.
15. Fesq HW, Bibby DM, Erasmus CS, Kable EJD, Sellschop JPF (1975) *Phys Chem Earth* 9:817–836.
16. Navon O, Hutcheon ID, Rossman GR, Wasserburg GJ (1988) *Nature* 335:784–789.
17. Schrauder M, Navon O (1994) *Geochim Cosmochim Acta* 58:761–771.
18. Izraeli ES, Harris JW, Navon O (2001) *Earth Planet Sci Lett* 187:323–332.
19. Klein-BenDavid O, Izraeli ES, Hauri E, Navon O (2004) *Lithos* 77:243–253.
20. Klein-BenDavid O, Wirth R, Navon O (2006) *Am Miner* 91:353–365.
21. Klein-BenDavid O, Izraeli ES, Hauri E, Navon O (2007) *Geochim Cosmochim Acta* 71:723–744.
22. Tomlinson EL, De Schrijver E, De Corte K, Jones AP, Moens L, Vanhaecke F (2005) *Geochim Cosmochim Acta* 69:4719–4732.
23. Tomlinson EL, Jones AP, Harris JW (2006) *Earth Planet Sci Lett* 250:581–595.
24. Schrauder M, Koeberl C, Navon O (1996) *Geochim Cosmochim Acta* 60:4711–4724.
25. Chrenko R, McDonald R, Darrow K (1967) *Nature* 214:474–476.
26. Zedgenizov DA, Kagi H, Shatsky VS, Sobolev NV (2004) *Miner Mag* 68(1):61–73.
27. Xu S, Okay AI, Ji S, Sengor AMC, Su W, Liu Y, Jiang L (1992) *Science* 256:80–92.
28. Yang J, Xu Z, Dobrzhinetskaya LF, Green HW, II, Pei X, Shi R, Wu C, Wooden JL, Zhang J, Wan Y, Li H (2003) *Terra Nova* 15:370–379.
29. Dobrzhinetskaya LF, Eide EA, Larsen RB, Sturt BA, Trønnes RG, Smith DC, Taylor WR, Posukhova TV (1995) *Geology* 23:597–600.
30. Massonne HJ (1999) *Proceedings of the Seventh Kimberlite Conference, Cape Town*, eds Gurney JJ, Gurney JL, Pascoe MD, Richardson SH (Red Roof Design, Cape Town, South Africa), pp 533–539.
31. Stöckhert B, Duyster J, Trepmann C, Massonne HJ (2001) *Geology* 29:391–394.
32. Mposkos E, Kostopoulos DK (2001) *Earth Planet Sci Lett* 192:497–506.
33. De Corte K, Cartigny P, Shatsky VS, Sobolev NV, Javoy M (1998) *Geochim Cosmochim Acta* 62:3765–3773.
34. De Corte K, Taylor WR, De Paepe P (2002) in *The Diamond-Bearing Kokchetav Massif, Kazakhstan*, eds Parkinson CD, Katayama I, Liou JG, Maruyama S (University Academy Press, Tokyo), pp 115–135.
35. Dobrzhinetskaya LF, Green HW, Mitchell TE, Dickerson RM, Bozhilov KN (2003) *J Metamorph Geol* 21:425–437.
36. Hwang S-L, Shen P, Chu H-T, Yui T-F, Liou JG, Sobolev NV, Shatsky VS (2005) *Earth Planet Sci Lett* 231:295–306.
37. Hwang SL, Chu HT, Yui TF, Shen P, Schertl HP, Liou JG, Sobolev NV (2006) *Earth Planet Sci Lett* 243:94–106.
38. Palyanov YN, Shatsky VS, Sokol AG, Tomilenko AA, Sobolev NV (2001) *Dokl Earth Sci* 381:935–939.
39. Shatsky VS, Palyanov YN, Sokol AG, Tomilenko AA, Sobolev NV (2005) *Int Geol Rev* 47:999–1010.
40. Sudo A, Tatsumi Y (1990) *Geophys Res Let* 17:29–32.
41. Harlow GE (1997) *Am Miner* 82:259–269.
42. Perchuk LL, Safonov OG, Yapaskurt VO, Barton JM, Jr (2002) *Lithos* 60:89–111.
43. Kamenetsky MB, Sobolev AV, Kamenetsky VS, Maas R, Danyushevsky LV, Thomas R, Pokhilenko NP, Sobolev NV (2004) *Geology* 32:845–848.
44. Maas R, Kamenetsky MB, Sobolev AV, Kamenetsky VS, Sobolev NV (2005) *Geology* 33:549–552.
45. Kamenetsky VS, Sharygin VV, Kamenetsky MB, Golovin AV (2006) *Geochem Int* 42:935–940.
46. Safonov OG, Perchuk LL, Litvin YA (2007) *Earth Planet Sci Lett* 253:112–128.
47. Montanini A, Harlov D (2006) *Lithos* 92:588–608.
48. Luth RW (2004) in *Treatise on Geochemistry*, eds Holland HD, Turekian KK (Elsevier, Amsterdam), pp 319–361.
49. Palyanov YN, Sokol AG, Sobolev NV (2005) *Russ Geol Geophys* 46:1271–1284.
50. Wang Y, Kanda H (1998) *Diam Relat Mater* 7:57–63.
51. Tomlinson E, Jones A, Milledge J (2004) *Lithos* 77:287–294.
52. Litvin YuA (2003) *Dokl Earth Sci* 389A:388–391.
53. Sokol AG, Tomilenko AA, Palyanov YN, Borzdov YuM, Palyanova GA, Khokhryakov AF (2000) *Eur J Miner* 12:367–375.
54. Kanda H, Fukunaga O (1982) in *High-Pressure Research in Geophysics*, eds Akimoto S, Manghnani MH (Academic, Tokyo) pp 525–535.
55. Palyanov YN, Sokol AG, Borzdov YuM, Khokhryakov AF, Shatsky AF, Sobolev NV (1999) *Diam Relat Mater* 8:1118–1124.
56. Shatsky AF, Borzdov YuM, Sokol AG, Palyanov YN (2002) *Geol Geofiz* 43:889–901.
57. Palyanov YN, Borzdov YuM, Kupriyanov IN, Gusev VA, Khokhryakov AF, Sokol AG (2001) *Diam Relat Mater* 10:2145–2152.
58. Palyanov YN, Borzdov YuM, Khokhryakov AF, Kupriyanov IN, Sobolev NV (2006) *Earth Planet Sci Lett* 250:269–280.
59. Palyanov YN, Sokol AG, Borzdov YuM, Khokhryakov AF, Sobolev NV (1999) *Nature* 400:417–418.
60. Palyanov YN, Sokol AG, Borzdov YuM, Khokhryakov AF (2002) *Lithos* 60:145–159.
61. Sokol AG, Palyanov YN, Palyanova GA, Khokhryakov AF, Borzdov YuM (2001) *Diam Relat Mater* 10:2131–2136.
62. Yamaoka S, Kumar MSD, Kanda H, Akaishi M (2002) *J Cryst Growth* 234:5–8.
63. Sokol AG, Palyanov YN (2004) *Geochemistry Int* 42:1018–1033.
64. Sokol AG, Palyanov YN, Palyanova GA, Tomilenko AA (2004) *Geochem Int* 42:830–839.
65. Luth RW (1999) in *Mantle Petrology: Field Observation and High-Pressure Experimentation: A Tribute to Francis R. (Joe) Boyd*, eds Fei Y, Bertka CM, Mysen BO (Geochem Soc, St. Louis), pp 297–316.
66. Ogasawara Y, Liou JG, Zhang RY (1997) *Geol Geofiz* 38:546–557.
67. Arima M, Kozai Y, Akaishi M (2002) *Geology* 30:691–694.
68. Palyanov YN, Sokol AG, Borzdov YuM, Khokhryakov AF, Sobolev NV (2002) *Am Miner* 87:1009–1013.
69. Palyanov YN, Sokol AG, Tomilenko AA, Sobolev NV (2005) *Eur J Miner* 17:207–214.
70. Siebert J, Guyot F, Malavergne V (2005) *Earth Planet Sci Lett* 229:205–216.
71. Gunn SC, Luth RW (2006) *Am Miner* 91:1110–1116.
72. Shatsky VS, Sobolev NV, Vavilov MA (1995) in *Ultrahigh Pressure Metamorphism*, eds Coleman RG, Wang X (Cambridge Univ Press, UK), pp 427–455.
73. Shatsky VS, Jagoutz E, Sobolev NV, Kozmenko OA, Parkhomenko VS, Troesch M (1999) *Contrib Miner Petrol* 137:185–205.
74. Shatsky VS, Ragozin AL, Sobolev NV (2006) *Russ Geol Geophys* 47:105–119.
75. Sobolev VS, Sobolev NV (1980) *Dokl Akad Nauk SSSR* 250:683–685.
76. Appleyard CM, Viljoen KS, Dobbe R (2004) *Lithos* 77:317–332.
77. Sobolev NV, Galimov EM, Smith CR, Yefimova ES, Maltsev KA, Hall AE, Usova LV (1989) *Geol Geofiz* 30:1–19.
78. Kaminsky FV, Zakharchenko OD, Griffin WL, Channer DMD, Khachatryan-Blinova GK (2000) *Can Miner* 38:1347–1370.
79. Shiryaev AA, Izraeli ES, Hauri EH, Zakharchenko OD, Navon O (2005) *Russ Geol Geophys* 46:1185–1201.
80. Kessel R, Ulmer P, Pettke T, Schmidt MW, Thompson AB (2005) *Earth Planet Sci Lett* 237:873–892.
81. Palyanov YN, Khokhryakov AF, Borzdov YuM, Sokol AG, Gusev VA, Rylov GM, Sobolev NV (1997) *Geol Geofiz* 38:882–904.